

Multihop Routing in Ad Hoc Networks

Don Torrieri*, Salvatore Talarico,[†] and Matthew C. Valenti[†]

*U.S. Army Research Laboratory, Adelphi, MD, USA.

[†]West Virginia University, Morgantown, WV, USA.

Abstract—This paper presents a dual method of closed-form analysis and lightweight simulation that enables an evaluation of the performance of mobile ad hoc networks that is more realistic, efficient, and accurate than those found in existing publications. Some features accommodated by the new analysis are shadowing, exclusion and guard zones, and distance-dependent fading. Three routing protocols are examined: least-delay, nearest-neighbor, and maximum-progress routing. The tradeoffs among the path reliabilities, average conditional delays, average conditional number of hops, and area spectral efficiencies are examined.

I. INTRODUCTION

There has been extensive recent research directed toward providing insights into the tradeoffs among the reliabilities, delays, and throughputs of mobile ad hoc networks with multihop routing (e.g., [1] - [5]). However, the mathematical models and necessary assumptions have not been adequate for obtaining reliable results. Much of this research uses network models based on stochastic geometry with the spatial distribution of the mobiles following a Poisson point process, and simplifying but unrealistic restrictions and assumptions. One of the principal problems associated with the models based on stochastic geometry [6], [7] is that they assume an infinitely large network with an infinite number of mobiles so that routing in the interior of the network cannot be distinguished from routing that includes a source or destination mobile near the perimeter of the network. The Poisson point process does not account for the dependencies in the placement of mobiles, such as the existence of exclusion zones [8] that ensure a minimum spatial separation between mobiles. Among the unrealistic restrictions are the absence of shadowing, the neglect of thermal noise, and the identical fading statistics for each link. Among the unrealistic assumptions are the independence of the success probabilities of paths from the source to the destination even when paths share the same links, and the constraining of the number of end-to-end retransmissions rather than link retransmissions.

This analysis in this paper combines closed-form calculations of outage probabilities, derived in [8], with simple and rapid simulations that accommodate additional network features. This approach allows routing to be statistically characterized without requiring assumptions about the statistical independence of possible paths. During each trial of the simulation, the topology is fixed and mobiles are placed according to any distribution; we focus on uniform clustering with exclusion and guard zones. Paths for message delivery are selected by using the closed-form expression for the per-link outage probability to determine which paths are possible, and the

delay associated with each available link is determined. The number of transmission attempts per link is constrained, and several routing protocols are considered. Using these paths and averaging over many topologies, three routing protocols are examined: least-delay, nearest-neighbor, and maximum-progress routing. The dependence of the path reliability, area spectral efficiency, average message delay, and average number of hops on network parameters such as the maximum number of transmission attempts per link, source-destination distance, and density of mobiles are evaluated.

Among the features of our analysis that distinguish it from those by other authors are the following.

1. Distinct links do not necessarily experience identically distributed fading.
2. Source-destination pairs are not assumed to be stochastically equivalent. For example if a source or destination is located near the perimeter of the network, the routing characteristics are different from those computed for source-destination pairs near the center of the network.
3. There is no assumption of independent path selection, path success probabilities, or link (hop) success probabilities. Many routes share links, which cause all these routes to fail if one of the shared links fails. Link success probabilities are correlated to the degree that lengths of the links are similar.
4. The shadowing over the link from one mobile to another can be modeled individually, as required by the local terrain. For computational simplicity in the examples, the shadowing is assumed to have a lognormal distribution.
5. The analysis accounts for the thermal noise, which is an important consideration when the mobile density, and hence the interference, is moderate or low.
6. The routing protocols do not depend on predetermined routes. Instead, they use the more realistic *dynamic route selection* that entails hop-by-hop route selection and allows for the possibility of successful communication over alternative routes.

II. NETWORK MODEL

The network comprises $M+2$ mobiles in a circular area with radius r_{net} , although any arbitrary two- or three-dimensional regions could be considered. The variable X_i represents both the i^{th} mobile and its location, and $\|X_i - X_j\|$ is the distance from the i^{th} mobile to the j^{th} mobile. Mobile X_0 serves as the reference transmitter or message source, and mobile X_{M+1} serves as the reference receiver or message destination. The other M mobiles X_1, \dots, X_M are potentially relays or sources of interference. Each mobile uses a single omnidirectional

antenna. The radii of the exclusion zones surrounding the mobiles are equal to r_{ex} .

The source and destination mobiles are placed within the circular area, and the remaining mobiles X_1, \dots, X_M are uniformly distributed throughout the network area outside the exclusion zones, according to a *uniform clustering* model. One by one, the location of each remaining X_i is drawn according to a uniform distribution within the radius- r_{net} circle. However, if an X_i falls within the exclusion zone of a previously placed mobile, then it has a new random location assigned to it as many times as necessary until it falls outside all exclusion zones. Setting the exclusion zone to $r_{\text{ex}} = 0$ is equivalent to drawing the mobiles from a binomial point process.

In a DS-CDMA network of asynchronous quadriphase direct-sequence systems, a multiple-access interference signal with power I before despreading is reduced after despreading to the power level $h(\tau_o)/G$, where G is the *processing gain* or *spreading factor*, and $h(\tau_o)$ is a function of the chip waveform and the timing offset τ_o of the interference spreading sequence relative to that of the desired or reference signal. If τ_o is assumed to have a uniform distribution over $[0, T_c]$, then the expected value of $h(\tau_o)$ is the chip factor h . For rectangular chip waveforms, $h = 2/3$ [9], [10]. It is assumed henceforth that $G/h(\tau_o)$ is a constant equal to G/h at each sector receiver in the network.

After the despreading, the power of X_i 's signal at the mobile X_j is

$$\rho_{i,j} = \tilde{P}_i g_{i,j} 10^{\xi_{i,j}/10} f(\|X_i - X_j\|) \quad (1)$$

where \tilde{P}_i is the received power at a reference distance d_0 (assumed to be sufficiently far that the signals are in the far field) after despreading when fading and shadowing are absent, $g_{i,j}$ is the power gain due to fading, $\xi_{i,j}$ is a shadowing factor, and $f(\cdot)$ is a path-loss function. The path-loss function is expressed as the power law

$$f(d) = \left(\frac{d}{d_0}\right)^{-\alpha}, \quad d \geq d_0 \quad (2)$$

where $\alpha \geq 2$ is the path-loss exponent. It is assumed that $r_{\text{ex}} \geq d_0$.

The $\{g_{i,j}\}$ are independent with unit-mean, but are not necessarily identically distributed; i.e., the channels from the different $\{X_i\}$ to X_j may undergo fading with different distributions. For analytical tractability and close agreement with measured fading statistics, Nakagami fading is assumed, and $g_{i,j} = a_{i,j}^2$, where $a_{i,j}$ is Nakagami with parameter $m_{i,j}$. When the channel between X_i and X_j undergoes Rayleigh fading, $m_{i,j} = 1$ and the corresponding $g_{i,j}$ is exponentially distributed. In the presence of shadowing with a lognormal distribution, the $\{\xi_{i,j}\}$ are independent zero-mean Gaussian with variance σ_s^2 . For ease of exposition, it is assumed that the shadowing variance is the same for the entire network, but the results may be easily generalized to allow for different shadowing variances over parts of the network. In the absence of shadowing, $\xi_{i,j} = 0$. It is assumed that the $\{g_{i,j}\}$ remain fixed for the duration of a time interval but vary independently

from interval to interval (block fading). We define μ_i to be the service probability that mobile i can serve as a relay along a path from a source to a destination. With probability p_i , the i^{th} mobile transmits in the same time interval as the desired signal. The $\{p_i\}$ can be used to model voice-activity factors, controlled silence, or failed link transmissions and the resulting retransmission attempts. When the j^{th} mobile is in service as a potential relay, we set $p_j = 0$.

The instantaneous signal-to-interference-and-noise ratio (SINR) at the mobile X_j of the signal transmitted by relay X_k is given by

$$\gamma_j = \frac{\rho_{k,j}}{\mathcal{N} + \sum_{i=1, i \neq k}^M I_i \rho_{i,j}} \quad (3)$$

where \mathcal{N} is the noise power, and the indicator I_i is a Bernoulli random variable with probability $P[I_i = 1] = p_i$ and $P[I_i = 0] = 1 - p_i$.

Since the despreading does not significantly affect the desired-signal power, the substitution of (1) and (2) into (3) yields

$$\gamma_j = \frac{g_{k,j} \Omega_{k,j}}{\Gamma^{-1} + \sum_{i=1, i \neq k}^M I_i g_{i,j} \Omega_{i,j}} \quad (4)$$

where

$$\Omega_{i,j} = \begin{cases} 10^{\xi_{k,j}/10} \|X_k - X_j\|^{-\alpha} & i = k \\ \frac{h P_i}{G P_k} 10^{\xi_{i,j}/10} \|X_i - X_j\|^{-\alpha} & i \neq k \end{cases} \quad (5)$$

is the normalized power of X_i at X_j , P_i is the received power from X_i at the reference distance d_0 before despreading when fading and shadowing are absent, and $\Gamma = d_0^\alpha P_k / \mathcal{N}$ is the SINR when relay X_k is at unit distance from mobile X_j and fading and shadowing are absent.

The *outage probability* quantifies the likelihood that the noise and interference will be too severe for useful communications. Outage probability is defined with respect to an SINR threshold β , which represents the minimum SINR required for reliable reception. In general, the value of β depends on the choice of coding and modulation. An *outage* occurs when the SINR falls below β .

In [8], closed-form expressions were found for the outage probability conditioned on the particular network geometry and shadowing factors. Let $\Omega_j = \{\Omega_{0,j}, \dots, \Omega_{M,j}\}$ represent the set of normalized powers at X_j . Conditioning on Ω_j , the *outage probability* of the link from relay X_k to receiver X_j is

$$\epsilon_{k,j} = P[\gamma_j \leq \beta | \Omega_j]. \quad (6)$$

The conditioning enables the calculation of the outage probability for any specific network geometry, which cannot be done by models based on stochastic geometry.

Restricting the Nakagami parameter $m_{k,j}$ of the channel between the relay X_k to receiver X_j to be integer-valued, the

outage probability conditioned on Ω_j is found in [8] to be

$$\epsilon_{k,j} = 1 - e^{-\beta_{k,j} z} \sum_{s=0}^{m_{k,j}-1} (\beta_{k,j} z)^s \sum_{t=0}^s \frac{z^{-t} H_{t,j}}{(s-t)!} \quad (7)$$

where $\beta_{k,j} = \beta m_{k,j} / \Omega_{k,j}$, $z = \Gamma^{-1}$,

$$H_{t,j} = \sum_{\ell_i \geq 0} \prod_{i=1, i \neq k}^M G_{\ell_i}(i, j) \quad (8)$$

$$\sum_{i=1}^M \ell_i = t$$

the summation in (8) is over all sets of indices that sum to t ,

$$G_{\ell}(i, j) = \begin{cases} 1 - p_i(1 - \Psi_{i,j}^{m_{i,j}}) & \text{for } \ell = 0 \\ \frac{p_i \Gamma(\ell + m_{i,j})}{\ell! \Gamma(m_{i,j})} \left(\frac{\Omega_{i,j}}{m_{i,j}} \right)^{\ell} \Psi_{i,j}^{m_{i,j} + \ell} & \text{for } \ell > 0 \end{cases} \quad (9)$$

and

$$\Psi_{i,j} = \left(\beta_{k,j} \frac{\Omega_{i,j}}{m_{i,j}} + 1 \right)^{-1} \quad \text{for } i = \{1, \dots, M\}. \quad (10)$$

III. ROUTING MODELS

There is no fixed optimal path from source X_0 to destination X_{M+1} in a network because every path has a nonzero probability of failure or outage. Link connectivity and end-to-end connectivity are random variables affected by the vicissitudes of fading. The optimal path, however defined, can change within milliseconds. There is one single-hop possible path from X_0 to X_{M+1} . There are M possible paths with 2 hops, $M(M-1)$ possible paths with no return to X_0 and 3 hops, and $O(M^{H-1})$ possible paths with no return to X_0 and H hops.

Three reactive or on-demand routing protocols are considered: *least-delay*, *nearest-neighbor*, and *maximum-progress routing*. All of these protocols only seek routes when needed. The medium-access-control protocol is Aloha or CSMA with collision avoidance. To simplify the analysis when CSMA is used, the CSMA guard zones are assumed to coincide with the exclusion zones.

In the implementation of least-delay routing, a source X_0 that seeks to communicate with a destination X_{M+1} floods the network with request packets to create it. The transmission of request packets through multiple routes increases the probability that some request packet successfully reaches the destination the failures of some paths. The path through intermediate relays followed by the packet that first reaches the destination determines the *least-delay path*, which conveys subsequent message packets, and subsequent receptions of other request packets by the destination are ignored. The least-delay path from X_0 to X_{M+1} causes the least interference throughout the network due to multiple transmissions of the same packet in a multihop path from X_0 to X_{M+1} .

In both nearest-neighbor and maximum-progress routing, the next relay in a path to the destination is dynamically selected at each hop of each packet and depends on the local configuration of available relays. A *candidate link* is one that connects available relays and is not experiencing an outage due to fading or unfavorable propagation conditions. Nearest-neighbor routing builds the *nearest-neighbor path* by choosing

the closest relay that lies at the end of a candidate link as the next one in the path from X_0 to X_{M+1} . Maximum-progress routing constructs the *maximum-progress path* by choosing the next relay on the path as the one that lies at the end of a candidate link and minimizes the remaining distance to the destination. In a practical implementation of either nearest-neighbor or maximum-progress routing, a geographic routing protocol would be used. *Geographic routing* [11] selects a path to a destination based on the geographic positions of the potential relays and makes path decisions at each hop. Each mobile must know its own location and the locations of other mobiles at the ends of candidate links. Both the nearest-neighbor and maximum-progress paths are among the successful paths from X_0 to X_{M+1} traversed by request packets during the flooding stage of least-delay routing.

Let $\delta(a, b)$ denote the distance between mobile a and mobile b . All routing methods use a *distance criterion* to exclude a link from mobile a to mobile b as a link in one of the possible paths from X_0 to X_{M+1} if $\delta(b, X_{M+1}) > \delta(a, X_{M+1})$. These exclusions, which will eliminate the majority of links, ensure that each possible path has links that always reduce the remaining distance to the destination. A mobile may not be able to serve as a relay in a path from X_0 to X_{M+1} because it is already receiving a transmission, is already serving as a relay in another path, is transmitting, or is otherwise unavailable. All links connected to mobiles that cannot serve as relays are excluded as links in possible paths from X_0 to X_{M+1} . Links that have not been excluded are called *included links*.

We draw a random realization of the network (topology) using the uniform clustering distribution of mobiles. Each network topology t is used in K_t simulation trials. The modeling of routing entails the identification of candidate links. Among the links between possible relays, the distance criterion is used to exclude various links, and we apply our analysis to determine the outage probability ϵ_i for each included link i . A Monte Carlo simulation uses the outage probabilities as failure probabilities to determine which of these links provides a successful transmission after B or fewer transmission attempts. Each included link that passes the latter test is called a *candidate link* and is assigned a delay determined by the number of transmission attempts N_i required for successful transmission, where $N_i \leq B$. The *candidate paths* from X_0 to X_{M+1} are paths that can be formed by using candidate links.

The *delay of candidate link* i is $T_i = N_i T + (N_i - 1) T_e$, where T is the *delay of a transmission over a link*, and T_e is the *excess delay* caused by a retransmission. The *delay* $T_{s,t}$ of a path from X_0 to X_{M+1} for network topology t and simulation trial s is the sum of the link delays in the path:

$$T_{s,t} = \sum_{i \in \mathcal{L}_{s,t}} [N_i T + (N_i - 1) T_e] \quad (11)$$

where $\mathcal{L}_{s,t}$ is the set of candidate links constituting the path, and the $\{T_{s,t}\}$ for topology t are sorted in ascending order of delay; i.e., $T_{s+1,t} \geq T_{s,t}$. If there is a routing failure, then $1/T_{s,t} = 0$.

A. Least-delay routing

For least-delay routing, the candidate path with the smallest delay from X_0 to X_{M+1} is selected as the *least-delay path* from X_0 to X_{M+1} . This path is determined by using the *Dijkstra algorithm* [12] with the candidate links and the cost of each link equal to the delay of the link. If there is no set of candidate links that allow a path from X_0 to X_{M+1} , then a *routing failure* occurs. If there are F_t routing failures for topology t and K_t simulation trials, then the *probability of end-to-end success* or *path reliability* within topology t is

$$R_t = 1 - \frac{F_t}{K_t}. \quad (12)$$

Among the $K_t - F_t$ trials with no routing failure, the *conditional average delay* from X_0 to X_{M+1} is

$$D_t = \frac{1}{K_t - F_t} \sum_{s=1}^{K_t - F_t} T_{s,t}. \quad (13)$$

If the least-delay path for trial s has h_{st} links or hops, then among the $K_t - F_t$ trials with no routing failure, the *conditional average number of hops* from X_0 to X_{M+1} is

$$H_t = \frac{1}{K_t - F_t} \sum_{s=1}^{K_t - F_t} h_{st}. \quad (14)$$

Let $\lambda = (M+1)/\pi r_{\text{net}}^2$ denote the density of transmitters in the network. We define the *normalized area spectral efficiency* for the K_t trials of topology t as

$$\mathcal{A}_t = \frac{\lambda}{K_t} \sum_{s=1}^{K_t} \frac{1}{T_{s,t}} \quad (15)$$

where the normalization is with respect to the bit rate or bits per channel use. The normalized area spectral efficiency is a measure of the end-to-end throughput in the network.

After computing R_t , D_t , H_t , and \mathcal{A}_t for Υ network topologies, we can average over the topologies to compute the *spatial averages*:

$$\begin{aligned} \bar{R} &= \frac{1}{\Upsilon} \sum_{t=1}^{\Upsilon} R_t, & \bar{D} &= \frac{1}{\Upsilon} \sum_{t=1}^{\Upsilon} D_t \\ \bar{H} &= \frac{1}{\Upsilon} \sum_{t=1}^{\Upsilon} H_t, & \bar{\mathcal{A}} &= \frac{1}{\Upsilon} \sum_{t=1}^{\Upsilon} \mathcal{A}_t. \end{aligned} \quad (16)$$

B. Nearest-neighbor routing

The candidate links are used to determine the nearest-neighbor path from X_0 to X_{M+1} . Starting with the source X_0 , the candidate link that spans the shortest Euclidean distance is selected as the first link in the nearest-neighbor path. The shortest link among the candidate links that are connected to the relay at the end of the previously selected link is added successively until the destination X_{M+1} is reached and, hence, the nearest-neighbor path has been determined. If no nearest-neighbor path from X_0 to X_{M+1} can be found, a routing failure is recorded. Equations (12)–(16) are used to determine the routing characteristics.

C. Maximum-progress routing

The candidate links are used to determine the maximum-progress path from X_0 to X_{M+1} . Starting with the source X_0 , the candidate link with a terminating relay that minimizes the remaining distance to destination X_{M+1} is selected as the first link in the maximum-progress path. The link among the candidate links that minimizes the remaining distance and is connected to the relay at the end of the previously selected link is added successively until the destination X_{M+1} is reached and, hence, the maximum-progress path has been determined. If no maximum-progress path from X_0 to X_{M+1} can be found, a routing failure is recorded. Equations (12) – (16) are used to determine the routing characteristics.

D. Simulation

In the dual approach of analysis and simulation, the simulation is simple and rapid because of the closed-form equation for the outage probability. The simulation allows the compilation of statistical characteristics of routing without assumptions about the statistical independence of possible paths. The simulation can be divided into three levels, each of which corresponds to a nested *for* loop. The outermost loop (Level 1) is run Υ times, once per topology. The next loop (Level 2) is run $\sqrt{K_t}$ times per topology, and the innermost loop (Level 3) is run $\sqrt{K_t}$ times for every iteration of level 2, so that the total number of trials per topology is K_t .

Level 1: Topology. The source mobile is placed at the origin, and the destination mobile is placed a distance $\delta(X_0, X_{M+1})$ from it. The other M mobiles are randomly placed according to the uniform clustering process.

Level 2: Service Model. Each of the M mobiles is marked as available as a relay with probability μ_i .

Level 3: Link-Level Simulation. The outage probability at each potential relay or destination is computed, where each mobile that is not a potential relay is a source of interference with probability p_i . By simulating outages, the candidate links are determined, and the required number of transmissions is determined for each of these links.

During each simulation trial, the least-delay, nearest-neighbor, and maximum-progress routes are identified.

IV. NUMERICAL RESULTS

Least-delay routing includes both the nearest-neighbor and maximum-progress paths among the candidate paths that could be selected by the Dijkstra algorithm. Thus, the least-delay path not only has less or equal delay than the nearest-neighbor and maximum-progress paths but also more or equal path reliability and area spectral efficiency.

In the subsequent examples of least-delay routing (LDR), nearest-neighbor routing (NNR), and maximum-progress routing (MPR), distances and times are normalized by setting $r_{\text{net}} = 1$ and $T = 1$. Other fixed parameter values are $r_{\text{ex}} = 0.05$, $T_e = 1$, $\Gamma = 0$ dB, $M = 200$, $K_t = 10^4$, and $\Upsilon = 1000$. Each power P_i is equal. A *distance-dependent fading* model is assumed, where a signal originating at mobile X_i arrives at mobile X_j with a Nakagami fading parameter

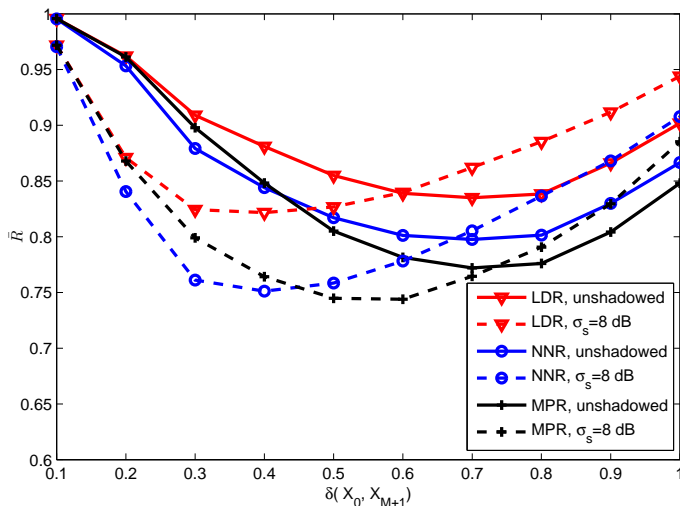


Fig. 1. Path reliability as a function of the distance between source and destination.

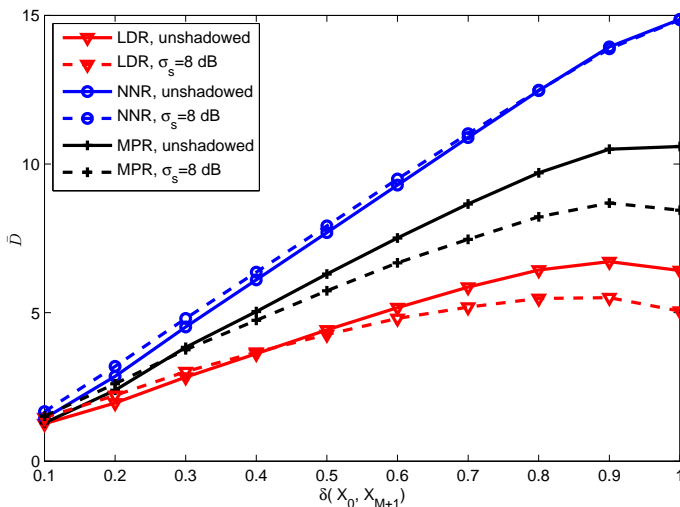


Fig. 2. Conditional average delay as a function of the distance between source and destination.

$m_{i,j}$ that depends on the distance between the mobiles. We set

$$m_{i,j} = \begin{cases} 3 & \text{if } \|X_j - X_i\| \leq r_f/2 \\ 2 & \text{if } r_f/2 < \|X_j - X_i\| \leq r_f \\ 1 & \text{if } \|X_j - X_i\| > r_f \end{cases} \quad (17)$$

where r_f is the *line-of-sight radius*. The distance-dependent-fading model characterizes the typical situation in which nearby mobiles are in each other's line-of-sight, while mobiles farther away from each other are not.

In Figures 1, 2, and 3, $\beta = 3$ dB, $B = 4$, $G/h = 48$, $\mu_i = 0.3$, $r_f = 0.2$, and $p_i = 0.4$. Figure 1 shows the variation of path reliability \bar{R} for each routing algorithm as the distance $\delta(X_0, X_{M+1})$ between the source X_0 and destination X_{M+1} increases. Plots are shown for both no shadowing and lognormal shadowing with $\sigma_s = 8$ dB, and $\alpha = 3.5$. For smaller values of $\delta(X_0, X_{M+1})$, the shadowing causes a decrease in path reliability, but the opposite is true for larger values. The increase in path reliability for larger values

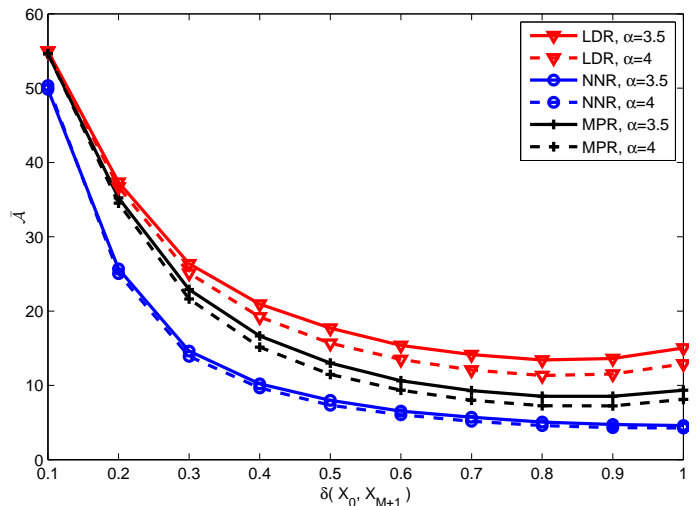


Fig. 3. Normalized area spectral efficiency as a function of the distance between source and destination.

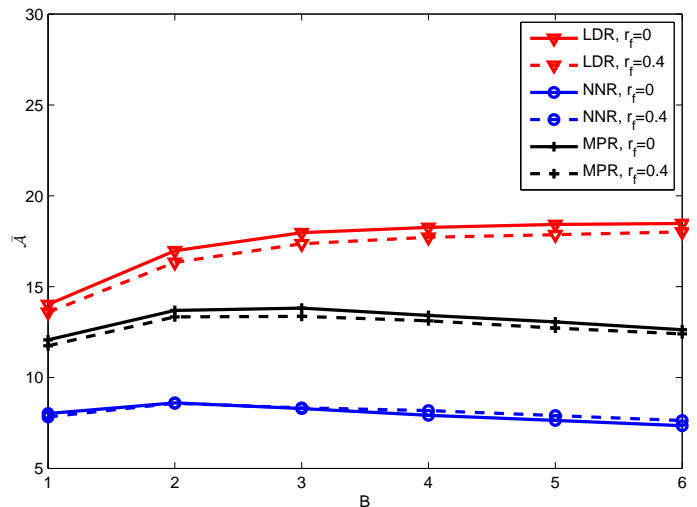


Fig. 4. Normalized area spectral efficiency as a function of the number of allowed transmissions.

of $\delta(X_0, X_{M+1})$, particularly with shadowing, is due to the decreased interference at the destination when it lies on the outskirts of the network. NNR exhibits greater path reliability than MPR if $\delta(X_0, X_{M+1}) > 0.45$.

Figure 2 shows the conditional average delay \bar{D} for each routing algorithm and $\alpha = 3.5$ as a function of $\delta(X_0, X_{M+1})$. For LDR and MPR and larger values of $\delta(X_0, X_{M+1})$, \bar{D} ceases to increase, and the shadowing causes an decrease in \bar{D} . For NNR, \bar{D} increases monotonically with $\delta(X_0, X_{M+1})$, and the shadowing has a relatively small effect. For $\delta(X_0, X_{M+1}) = 1$ and shadowing, it is found that $\bar{H} \approx 2.0, 2.4,$ and 7.3 for LDR, MPR, and NNR, respectively.

Figure 3 shows the normalized area spectral efficiency \bar{A} for each routing algorithm as a function of $\delta(X_0, X_{M+1})$ with α as a parameter. Shadowing with $\sigma_s = 8$ dB is assumed. As α increases, both the desired signal and the interference signals are attenuated. However, particularly for large $\delta(X_0, X_{M+1})$, the net effect is that the more severe propagation conditions reduce \bar{A} , which is largest for LDR and least for NNR.

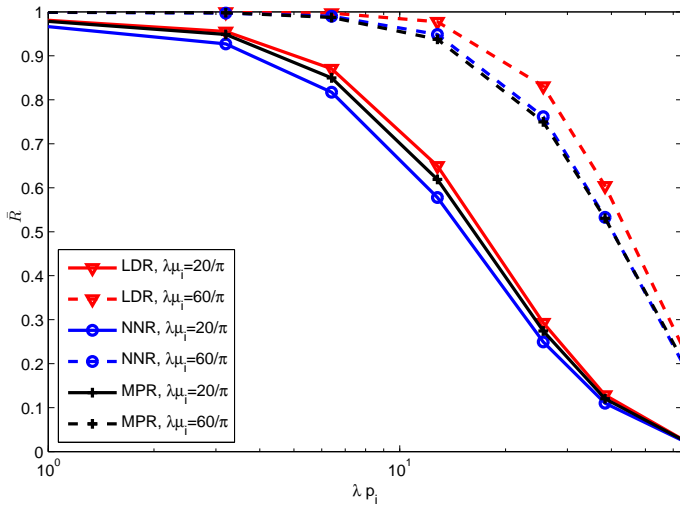


Fig. 6. Path reliability as a function of contention density.

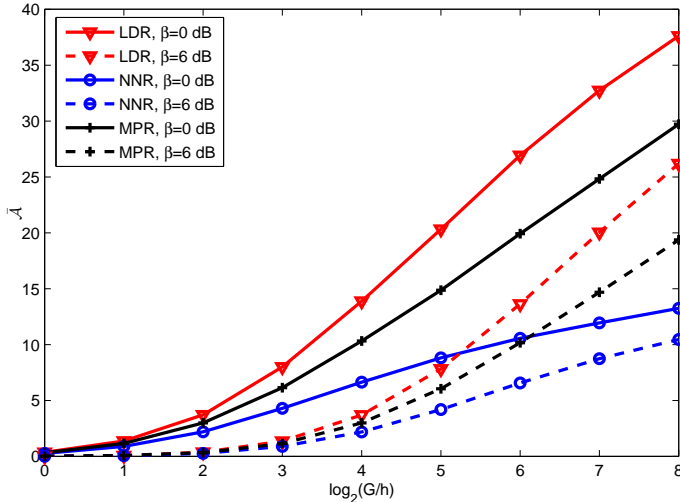


Fig. 5. Normalized area spectral efficiency as a function of the spreading factor.

When the number of allowed transmission attempts B increases, the path reliability and conditional average delay increase for all three routing algorithms. Figure 4 shows the normalized area spectral efficiency \bar{A} for each routing algorithm as a function of B with the line-of-sight radius r_f as a parameter. The parameter values are $\beta = 3$ dB, $\alpha = 3.5$, $\delta(X_0, X_{M+1}) = 0.5$, $G/h = 48$, $\mu_i = 0.3$, and $p_i = 0.4$. Little or no increase in \bar{A} occurs beyond $B = 2$. The reason is that more allowed transmissions not only provide greater path reliability but also lead to successful paths with longer delays. An increase in r_f is slightly detrimental.

The effects of the spreading factor G and the SINR threshold β are illustrated in Figure 5. All other parameter values are the same as those in Figure 4 except that $r_f = 0.2$, and $B = 4$. The normalized area spectral efficiency \bar{A} increases monotonically with G . An increase in β affects LDR and MPR

more than NNR.

Figure 6 shows the path reliability for each routing protocol as a function of the contention density λp_i with relay density $\lambda \mu_i$ as a parameter. This figure indicates the degree to which an increase in the contention density is mitigated by an increase in relay density.

V. CONCLUSIONS

This paper presents a new analysis of multihop routing in ad hoc networks. Many unrealistic and improbable assumptions and restrictions of existing analyses are discarded. The new analysis is combined with a simulation to compare three routing protocols: least-delay, nearest-neighbor, and maximum-progress routing. The tradeoffs among the path reliabilities, average delays, and area spectral efficiencies of these three routing protocols and the effects of various parameters have been shown. Least-delay routing has superior characteristics, but its overhead cost is large because it requires flooding. Maximum-progress and nearest-neighbor routing both have much lower overhead costs, but provide more conditional average delay, less area spectral efficiency, and less path reliability than least-delay routing. Maximum-progress routing provides less conditional average delay and more area spectral efficiency than nearest-neighbor routing, but provides less path reliability when the paths are long.

REFERENCES

- [1] Y. Chen and J. G. Andrews, "An Upper Bound on Multihop Transmission Capacity With Dynamic Routing Selection," *IEEE Trans. Inform. Theory*, vol. 58, pp. 3751-3765, June 2012.
- [2] P. H. J. Nardelli, M. Kaynia, P. Cardieri, and M. Latva-aho, "Optimal Transmission Capacity of Ad Hoc Networks with Packet Retransmissions," *IEEE Trans. Wireless Commun.*, vol. 11, pp. 2760-2766, Aug. 2012.
- [3] P. H. J. Nardelli, and M. Latva-aho, "Efficiency of Wireless Networks under Different Hopping Strategies," *IEEE Trans. Wireless Commun.*, vol. 11, pp. 15-20, Jan. 2012.
- [4] R. Vaze, "Throughput-delay-reliability tradeoff with ARQ in wireless ad hoc networks," *IEEE Trans. Wireless Commun.*, vol. 10, pp. 2142-2149, July 2011.
- [5] J. G. Andrews, S. Weber, M. Kountouris, and M. Haenggi, "Random access transport capacity," *IEEE Trans. Wireless Commun.*, vol. 9, pp. 2101-2111, June 2010.
- [6] D. Stoyan, W. Kendall, and J. Mecke, *Stochastic Geometry and its Applications*, 2nd ed., Wiley, 1996.
- [7] S. Weber, J. G. Andrews, and N. Jindal, "An overview of the transmission capacity of wireless networks," *IEEE Trans. Commun.*, vol. 58, pp. 3593-3604, Dec. 2010.
- [8] D. Torrieri and M. C. Valenti, "The outage probability of a finite ad hoc network in Nakagami fading," *IEEE Trans. Commun.*, vol. 60, pp. 3509-3518, Nov. 2012.
- [9] D. Torrieri, *Principles of Spread-Spectrum Communication Systems*, 2nd ed. Springer, 2011.
- [10] D. Torrieri, "Performance of direct-sequence systems with long pseudonoise sequences," *IEEE J. Selected Areas Commun.*, vol. 10, pp. 770-781, May 1992.
- [11] F. Cadger, K. Curran, J. Santos, and S. Moffett, "A Survey of Geographical Routing in Wireless Ad-Hoc Networks," *IEEE Commun. Surveys Tut.*, vol. 15, pp. 621-653, second quarter, 2013.
- [12] R. A. Brualdi, *Introductory Combinatorics*, 5th ed., Pearson Prentice Hall, 2010.